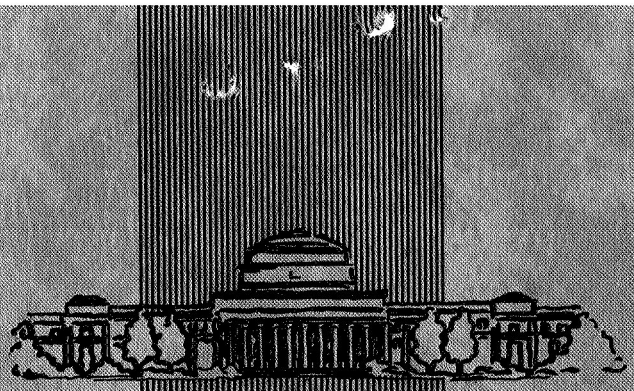

MASSACHUSETTS INSTITUTE OF TECHNOLOGY

RE-43

ANALYSIS OF ERROR PROPAGATION IN AIRCRAFT INERTIAL NAVIGATION SYSTEMS

by

John C. Ruth

July 1968

EXPERIMENTAL ASTRONOMY LABORATORY
MASSACHUSETTS INSTITUTE OF TECHNOLOGY
CAMBRIDGE 39, MASSACHUSETTS

RE-43

ANALYSIS OF ERROR PROPAGATION IN AIRCRAFT INERTIAL NAVIGATION SYSTEMS

by

John C. Ruth

July 1968

Approved: W. Markey

Director,
Experimental Astronomy Laboratory

ABSTRACT

An analysis is presented of the dominant sources of error in three different aircraft inertial navigation systems. The three systems studied, all of which are undamped, are:

1) A local-level, free azimuth system
2) A space-stabilized system
3) A strap-down system

Linearized mathematical error models describe each system, while the use of a digital computer is necessary to perform the required simulations.

Various flight paths and maneuvers are simulated, and the position errors are analyzed on the basis of the sources contributing to the error. It is assumed that the sources of the errors are contained in the instruments mounted in each system. The error models representing the gyros and accelerometers for each system are described in the paper. The gyros are assumed to be of the single-degree-of-freedeom, floated, integrating type; and the accelerometers are assumed to be of the pulsed, integrating, floated, pendulum type. The effects of gravitational attraction, inertial acceleration, linear velocity, angular velocity, and angular acceleration on the position error of the systems are presented and analyzed. The factor of elapsed time, short duration missions versus long duration missions, is discussed. The dominant sources of error for the various systems are identified and analyzed.

For the specific systems studied in this paper, conclusions are drawn pertaining to the value gained by flight testing of these systems. It is shown that the effects of the dynamics of the flight path on the systems' performance do not produce the dominant terms, forcing the position errors. In fact, adequate knowledge of the systems' performance may be gained by laboratory and van-road testing of the system. It is shown that the dominant error sources are primarily affected by gravitational attraction and elapsed time; therefore, the additional costs of flight testing systems of these types for performance parameters appear to be unjustified.

It is realized that certain assumptions made in the development of this topic may influence the results. However, the assumptions and their possible ramifications on the systems' performance are discussed.

ACKNOWLEDGMENTS

This report was prepared under DSR Project 70343 sponsored by the National Aeronautics and Space Administration Electronic Research Center, Cambridge, Massachusetts, through NASA Grant No. NGR 22-009-229.

The publication of this report does not constitute approval by the National Aeronautics and Space Administration or by the MIT Experimental Astronomy Laboratory of the findings or the conclusions contained therein. It is published only for the exchange and stimulation of ideas.

TABLE OF CONTENTS

Introduction

An analysis is presented of the dominant sources of error in three different inertial navigation systems. The three systems studied, all of which are undamped, are:

1) A local-level, free azimuth system
2) A space-stabilized system
3) A strap-down system

Linearized mathematical error models [1]* describe each system, and the necessary simulations are performed with the aid of an electronic computer. Figures 1-1, 1-2, and 1-3 illustrate the functional diagrams of the systems under study. Note the unique mechanization of the local-level free azimuth system. The navigation computer solves the first order differential equation $\dot{\bar{h}}_L = \bar{r} \times \bar{a}$. $\dot{\bar{h}}_L$ is the derivative of the vehicle's angular momentum taken with respect to the rotating platform, $\bar{r}$ is the vehicle's position vector, and $\bar{a}$ (which is $\ddot{\bar{r}} - \bar{G}$) is the quantity sensed by an accelerometer on the rotating platform. This mechanization does not require an explicit term which corresponds to the Coriolis correction of the more conventional navigation equations. A complete derivation is provided in Appendix A, Section 2, of Ref. 1.

Assumptions

Many assumptions are made in the development of this paper, and it is appropriate to discuss them at this point. Since only comparisons among the three systems are intended, a spherical, non-rotating earth is assumed in all computer simulations. The absence of the earth's rotational vector presents no difficulties as none of the system mechanizations are required to track this vector. While the fact that the earth is not a sphere does require in actual systems certain compensations for the navigational equations, the results of the computer simulations represent deviations from the nominal flight path without regard to the actual flight path.

The navigational computer on board the aircraft is assumed to be a perfect device, and all errors in the various systems are assumed to be due to the instruments. The gyroscopes are assumed to be of the single-degree-of-freedom, floated, integrating type; the accelerometers are assumed to be of the pulsed, integrating, floated, pendulum type. All of the navigational system components are assumed to operate in a pulsed, digital mode.

---

*Numbers in brackets denote references found on page 7.

This paper has concentrated on the instrument error sources and has neglected the error sources which are associated with the system alignment and initial conditions. An error model is postulated for the instruments used in the various mechanizations. Table 1 lists the specific gyroscope error model utilized in the simulations. The values of the error coefficients were selected arbitrarily but were given realistic values which would approximate a .1 meru rated gyroscope. The rating of .1 meru is defined to be the root-mean-squared deviation of one test error curve as compared to the previous test error curve on a continuously running test cycle. The error coefficients used are the residual uncertainty remaining after compensation has been applied after a calibration check. These residual uncertainties can be considered to be time-varying, random, and unknown. However, a statistical description of these uncertainties is assumed. Based on a seven-day recalibration cycle, all values are one sigma standard deviation, all error sources being uncorrelated. Table 2 lists the specific accelerometer error model utilized in the simulations. The accelerometers modeled were of very high quality with an uncertainty in the range of four parts per million. It is assumed that all of the instruments used in a specific mechanization are identical.

A perfect altimeter is assumed in each of the systems whereby, at the end of each integration step of the navigational computer, a correction is applied to the vertical component of the position vector. In this manner divergence of the computations in the vertical channel is precluded. Obviously, no accelerometer is required in the vertical channel of the local vertical mechanization.

The position errors, given in units of feet, are displayed in north and east coordinates with time given in seconds. Since each error source is assumed to be uncorrelated, the total system position error is just the square root of the sum of the squares of each individual error source.

Simulated Flight Profiles

Four different missions were simulated in order to observe the error propagation under various conditions. For the details of the four simulations, please refer to:

Table 3 - Simulated Mission #1

Table 4 - Simulated Mission #2

Table 5 - Simulated Mission #3

Table 6 - Simulated Mission #4

Mission #1 shows a typical reconnaissance mission by a helicopter. It takes off on a northeast heading, climbs to altitude, travels for a short period of time, and then hovers. It then accelerates in a northwesterly direction and executes a high-speed turn back to a northeasterly heading. There is a two-phase deceleration after which the simulation concludes with the helicopter in the hover state.

Mission #2 depicts a tactical fighter which takes off on an easterly heading and climbs to altitude. It attains a high velocity, dives, and decelerates while leveling off. It remains at the lower altitude, decelerates, and then makes an 180° constant velocity turn. As it approaches a landing field, it decelerates and lands.

Mission #3 illustrates a supersonic transport flying east with a small northerly component of velocity. No maneuvers are performed except those necessary due to the curvature of the earth. The mission terminates in this state after ten hours.

Mission #4 is a test aircraft which takes off on a northeast heading and climbs to altitude. It proceeds for 42 minutes, does a sharp 180° turn, flies a 42-minute southwest leg, and then makes another sharp 180° turn. There is a 42-minute northeast leg followed by another 180° turn. The mission terminates after flying 42 minutes more on the southwest heading.

It is obvious that the assumed missions constitute a relatively benign flight profile since buffeting and other vibrational effects are neglected. Recent studies in the laboratory and on test sleds indicate that a vibrational environment should not seriously degrade a strap-down system.[2] However, one must keep in mind the environment experienced when assessing the final results.

The missions start on the equator, and all systems are initially aligned to the geographic coordinates, north, east, and down. The two gyroscopes in the horizontal plane are oriented with their output axes initially along down, parallel to the local gravity vector. The local-level, free azimuth system maintains its orientation during the simulated missions. The space-stabilized system, being fixed in inertial space, will tend to rotate with respect to the local gravity vector as the platform moves over the spherical earth. The strap-down system, being body-fixed, will tend to rotate with respect to the local gravity vector as a function of vehicle attitude.

Results

In all of the simulations, certain common characteristics

were noted. For approximately the first ten minutes of each simulated mission, the horizontal accelerometers provide the dominant error sources for the system position errors. The assumed error coefficients are such that the bias term of the horizontal accelerometers is the dominant error source unless there have been sustained accelerations of over one "g," in which case the scale factor term tends to dominate. Since the accelerometer-induced errors oscillate at the Schuler frequency, they are bounded with a maximum value dependent upon the size of the error coefficient and the dynamics of the flight path. The length of time in which the accelerometers exert their dominance is determined by the same two factors--the size of the error coefficients and the dynamics of the flight path. As a test of this philosophy, an accelerometer with error coefficients one order of magnitude larger was substituted in one of the simulations. In this case the accelerometer dominance was extended to approximately the first 35 minutes of the flight.

After this initial period of dominance by the accelerometers, the gyroscopes take over and become the dominant position error sources for the remainder of the mission. Depending on the specific mission flown, a number of error sources contribute to the total error; but, as time progresses, two of the error sources totally dominate. After approximately 2,000 seconds, the space-stabilized and local-level systems' dominant error sources are the bias term and the output axis linear term of the nominally horizontal gyroscopes. The strap-down system also shows this characteristic; but, in addition, there is a contribution from the nominally vertical gyroscope's input axis linear term. This contribution is dependent upon the aircraft's attitude with respect to the vertical. After approximately three hours, the space-stabilized system's dominant error sources begin to switch from one gyroscope to another gyroscope as a function of the specific flight path flown. With the exception of the local-level system, the gyroscope's orientation with respect to the local gravity vector is an important factor in determining the dominant error source.

Please refer to Figures 1-4 through 1-10 for graphs illustrating the total system position errors along north and east. Included are the plots of the various dominant error source contributions.

Discussion

It is interesting to note that the gyroscopes are the dominant error sources for these systems during the majority of anticipated aircraft flight times. Unless the accelerometers are of exceedingly low quality, their role in determining the

dominant error sources is limited to the early portions of the flight mission. Yet it was not solely the dynamics of the flight path which determined the dominant error sources. The factors of time and gravitational attraction cause certain error sources to dominate.

The gyroscope's bias term produces a position error which is only a function of time. The simulations show this error to be composed of a ramp with an approximately 124-foot Schuler component superimposed. The slope of the ramp is approximately .152 feet per second. Britting and Smith [3] derive analytical error equations for the space-stabilized system assuming constant gyroscope drift. Since the bias term can be thought of as a constant drift term, the position error due to the bias term is found to be the same from the linearized simulations as from the analytically derived equations.

In the local-level system the output axis of the horizontal gyroscopes and the input axis of the vertical gyroscope feel a constant gravitational attraction force of one "g" throughout the duration of the flight. With a constant input this error source produces position errors in exactly the same manner as the bias term. Again the constant drift generates a ramp with a superimposed Schuler component. However, the slope of the ramp and the height of the Schuler are larger because the error coefficient is 50 percent larger. Had a different error coefficient been assumed for these values, the position errors due to them would have been changed accordingly. In the error graphs 1-4 through 1-10, the total position error is shown and the effect of the gyroscope's bias error term illustrated. By taking the square root of the sum of the squares of the bias and linear terms, one may account for approximately 97 percent of the total system error.

In the space-stabilized and strap-down systems, the instruments' orientation with respect to the local gravity vector influences the source of error contributions in the two display coordinates. In this instance the errors are shifted from the computational coordinate frame (inertial) to the display coordinates as a function of the instruments' orientation. This accounts for the case of an originally vertical gyroscope in the space-stabilized system later becoming a horizontal gyroscope. During the interim both instruments share in the error contributions of the display coordinates. Another phenomenon which became apparent during this study was an "averaging" process caused by rotations of the instrument with respect to the specific force vector acting on the platform. The strap-down system appeared to perform better in those instances involving turns because the error model simulation integrates algebraically, taking into account the sign of the error forcing input. This algebraic averaging process is again noted in a

long-term sense when the space-stabilized system slowly tumbled with respect to the local gravity vector in the ten-hour Mission #3. Unfortunately, the local-level system was not able to take advantage of any of these averaging phenomena.

All the error sources which are affected by inertial acceleration, linear velocity, angular velocity, and angular acceleration, did contribute to the total error propagation. For the missions described in this paper, however, the flight dynamics produced position errors which were at least an order of magnitude smaller than those produced by the two dominant sources. The dominant error sources are flight-path independent, and an inertial navigator would generate approximately the same position errors if it were stationary.

It is conceivable that the system alignment and initial condition errors could in fact be the dominant system position errors. For the purposes of this analysis, however, only the instrument errors were evaluated. There is a correlation between certain instrument error sources and the alignment error sources, but again this was ignored for this analysis.

Conclusions

It is concluded that the effects of the flight dynamics on the specific systems studied in this paper are normally insignificant; therefore, little additional knowledge is gained by an extensive flight test program. It is also concluded that adequate knowledge of the systems' performance can be gained by laboratory test-bench and van-road testing of the systems. The assumption by many authors of constant gyro drift error models appears to be justified for analytical studies involving complicated flight paths. The additional costs of flight test programs appear to be unjustified when testing systems of the type described in this paper. The buffeting and vibrational effects on a strap-down inertial navigation system are not fully known; therefore, the above stated conclusions should be tempered by the relatively benign flight profiles simulated.

References

1. Ruth, J. C., "A Parametric Comparison of Aircraft Inertial Navigation Systems," Air Force Missile Development Center Technical Report MDC-TR-67-22 Project 5177, Holloman Air Force Base, New Mexico, June 1967.

2. Lorenzini, D. A., Beggs, L. D., Ingold, N. L., Simaitis, E., "Laboratory and Sled Tests of the Lunar Excursion Module Abort Sensor Assembly (Strapped-Down Inertial Measurement Unit)," Project 681D, MDC-TR-68-11, AFMDC Central Inertial Guidance Test Facility, Holloman Air Force Base, New Mexico, February 1968.

3. Britting, K. R., and Smith, M. A., "Effect of Gyro Drift in an Inertial Navigation System in which the Stable Member is Assumed to be Inertially Nonrotating," Instrumentation Laboratory Report E-1661, MIT, Cambridge, Massachusetts, July 1964.

TABLE 1. GYRO ERROR MODEL COEFFICIENTS*

ERROR COEFFICIENT FOR:	UNITS	MECHANIZATION		
		Space-Stabilized	Local-Vertical	Strap-Down
Bias	Meru	.1	.1	.1
Scale Factor	μMeru/Meru	0	2	2
Acceleration along input axis	Meru/g	.3	.3	.3
Acceleration along output axis	Meru/g	.15	.15	.15
Acceleration along spin axis	Meru/g	.15	.15	.15
Acceleration squared, along input axis	$Meru/g^2$	.1	.1	.1
Acceleration squared, along spin axis	$Meru/g^2$	.1	.1	.1
Acceleration product, along input axis and output axis	$Meru/g^2$	.1	.1	.1
Acceleration product, along input axis and spin axis (major compliance)	$Meru/g^2$	.1	.1	.1
Acceleration product, along output axis and spin axis	$Meru/g^2$	.1	.1	.1
The following error sources are a function of the environment experienced by the strapdown instruments.				
Anisoinertia term	$Meru/(rad/sec)^2$			.1
Output axis angular acceleration	$Meru/rad/sec^2$			30
Quadratic rotational cross coupling	$Meru/(rad/sec)^2$			.08
Linear cross coupling	$Meru/(rad/sec)^2$			.6

*All values are one sigma standard deviation, based on a seven-day recalibration cycle.

TABLE 2

ACCELEROMETER ERROR MODEL COEFFICIENTS*

ERROR COEFFICIENT FOR:	UNITS	MECHANIZATION		
		Space-Stabilized	Local-Vertical	Strap-Down
Bias	μg	1	1	1
Acceleration, along input axis	μg/g	4	4	4
Acceleration squared, along input axis	$\mu g/g^2$	.1	.1	.1
The following error sources are a function of the environment experienced by the strap-down instruments.				
Anisoinertia	$\mu g/(rad/sec)^2$			100
Output axis angular acceleration	$\mu g/rad/sec^2$			50
Quadratric rotational cross coupling	$\mu g/(rad/sec)^2$			1
Linear cross coupling	$\mu g/g^2$			1

*All values are one sigma standard deviation, based on a seven-day recalibration cycle.

TABLE 3

SIMULATED MISSION NUMBER 1

SEQUENCE OF MANEUVERS

Starting time in seconds	Duration in seconds	Acceleration in g's	ω about roll axis in rad/sec	ω about pitch axis in rad/sec
0	7.5	.25		
0	16	.25		
0	6			.125
8	7.5			-.100
8	7.5	-.25		
706	16	-.25		
782	31	.0001575		
782	31			
1083	20	.25		
4673	16	.5		
4673	3		.15	.03
4676	10			.0388
4686	3		-.15	.03
4689	10	-.25		
5029	10	-.25		
5410	Terminate this mission in the hover state			

TABLE 3

SIMULATED MISSION NUMBER 1

SEQUENCE OF MANEUVERS

ω about yaw axis in rad/sec	Velocity attained at end in feet per second	Altitude attained at end in feet	Description of maneuver
			Vertical
			Horizontal
			Pitch
			Level off
	128	482	Vertical
	.1	482	Horizontal
			Turn
-.0509	.1	482	About yaw
	160	482	Horizontal
			Turn
.1			Turn-roll
.0894			Turn
.1	160	482	Turn-roll
	80	482	Horizontal
	.1	482	Horizontal

TABLE 4

SIMULATED MISSION NUMBER 2

SEQUENCE OF MANEUVERS

Starting time in seconds	Duration in seconds	Acceleration in g's	ω about roll axis in rad/sec	ω about pitch axis in rad/sec
0	40	.25		
20	10	.5		
20	6			.1
70	20	-.25		
70	10	.25		
80	10			-.06
270	10	2		
520	5	-1		
520	5	-1		
520	3			-.1
555	3			.1
555	5	1		
1160	10	-2		
1290	40	.58		
1290	5		-.10	.01966
1295	30			.03927
1325	5		.10	.01966
2260	10	-.25		
2260	3			-.100
2300	10	.25		
2300	30	-.25		
2300	6			.05
2340	Terminate this mission at landing site			

TABLE 4

SIMULATED MISSION NUMBER 2

SEQUENCE OF MANEUVERS

ω about yaw axis in rad/sec	Velocity attained at end in feet per second	Altitude attained at end in feet	Description of maneuver
			Horizontal
			Vertical
			Pitch up
			Vertical
			Horizontal
	402	8848	Level off
	1045	8848	Horizontal
			Horizontal
			Vertical
			Pitch down
			Level out
	884	3217	Vertical
	241	3217	Horizontal
			Turn
-.076			Turn-roll
-.068			Turn
-.076	241	3217	Turn-roll
			Vertical
	254	2815	Pitch down
			Vertical
			Horizontal
	.1	0	Level off

TABLE 5

SIMULATED MISSION NUMBER 3

SEQUENCE OF MANEUVERS

Starting time in seconds	Duration in seconds	Acceleration in g's	ω about roll axis in rad/sec	ω about pitch axis in rad/sec
0	36,000			
0	36,000			-.0000735
36,000	Terminate this mission in constant velocity state			

TABLE 5

SIMULATED MISSION NUMBER 3

SEQUENCE OF MANEUVERS

ω about yaw axis in rad/sec	Velocity attained at end in feet per second	Altitude attained at end in feet	Description of maneuver
	1533	40,000	Constant velocity
	1533	40,000	Slow pitch

TABLE 6

SIMULATED MISSION NUMBER 4

SEQUENCE OF MANEUVERS

Starting time in seconds	Duration in seconds	Acceleration in g's	ω about roll axis in rad/sec	ω about pitch axis in rad/sec
0	50	.25		
20	15	.5		
20	10			.08
110	20			-.04
110	30	-.25		
110	11	1.5		
2660	30	3		
2660	15		-.08	.0676
2675	15		.08	.0676
5210	30	3		
5210	15		-.08	.0676
5225	15		.08	.0676
7760	30	3		
7760	15		-.08	.0676
7775	15		.08	.0676
10,400	Terminate this mission at landing site			

TABLE 6

SIMULATED MISSION NUMBER 4

SEQUENCE OF MANEUVERS

ω about yaw axis in rad/sec	Velocity attained at end in feet per second	Altitude attained at end in feet	Description of maneuver
			Horizontal
			Vertical
			Pitch up
			Level off
			Vertical
	933	23,526	Horizontal
			Turn
-.085			Turn-roll
-.085	933	23,526	Turn-roll
			Turn
-.085			Turn-roll
-.085	933	23,526	Turn-roll
			Turn
-.085			Turn-roll
-.085	933	23,526	Turn-roll

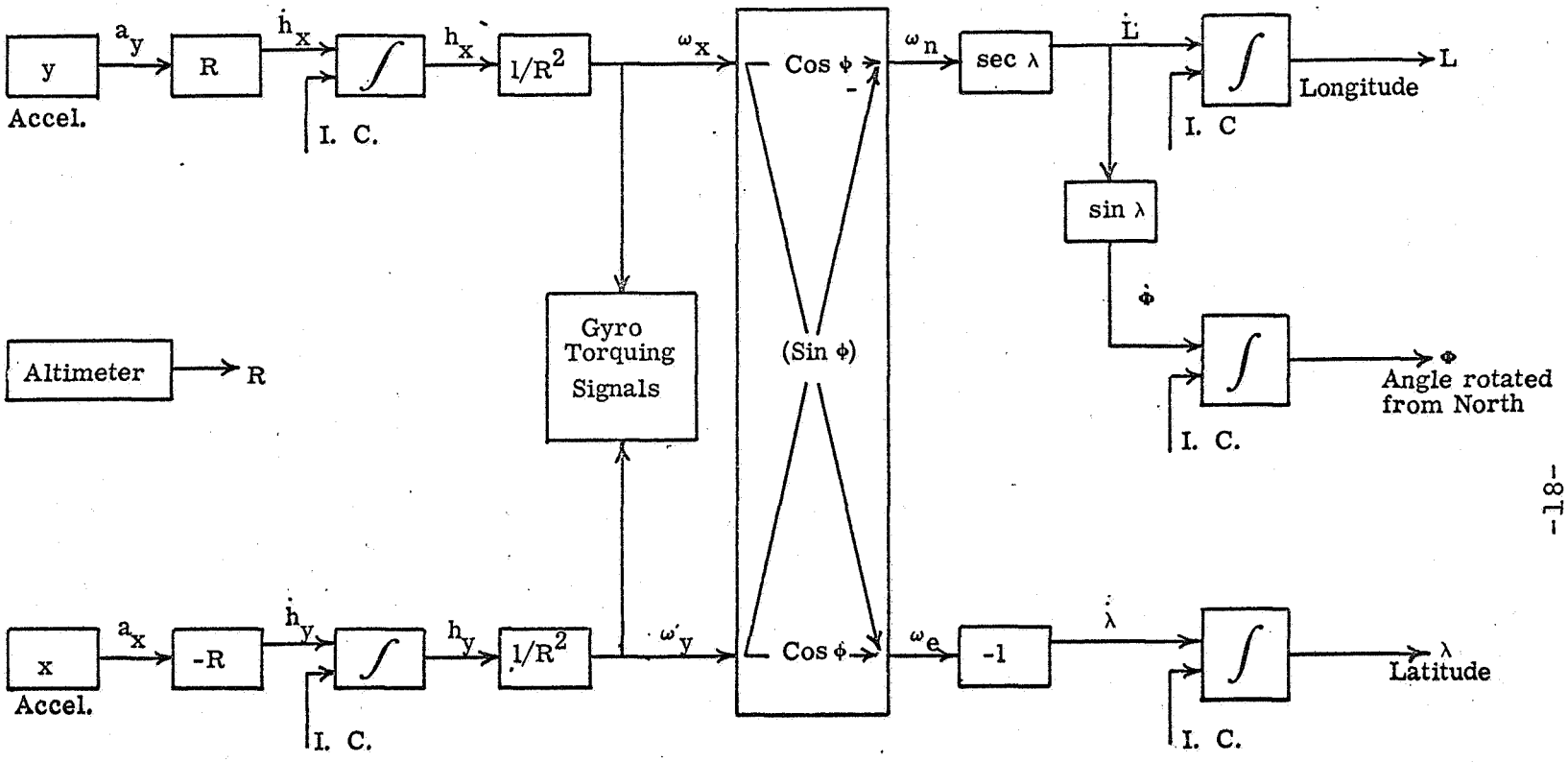

BLOCK DIAGRAM OF THE LOCAL VERTICAL SYSTEM

FIG. 1-1

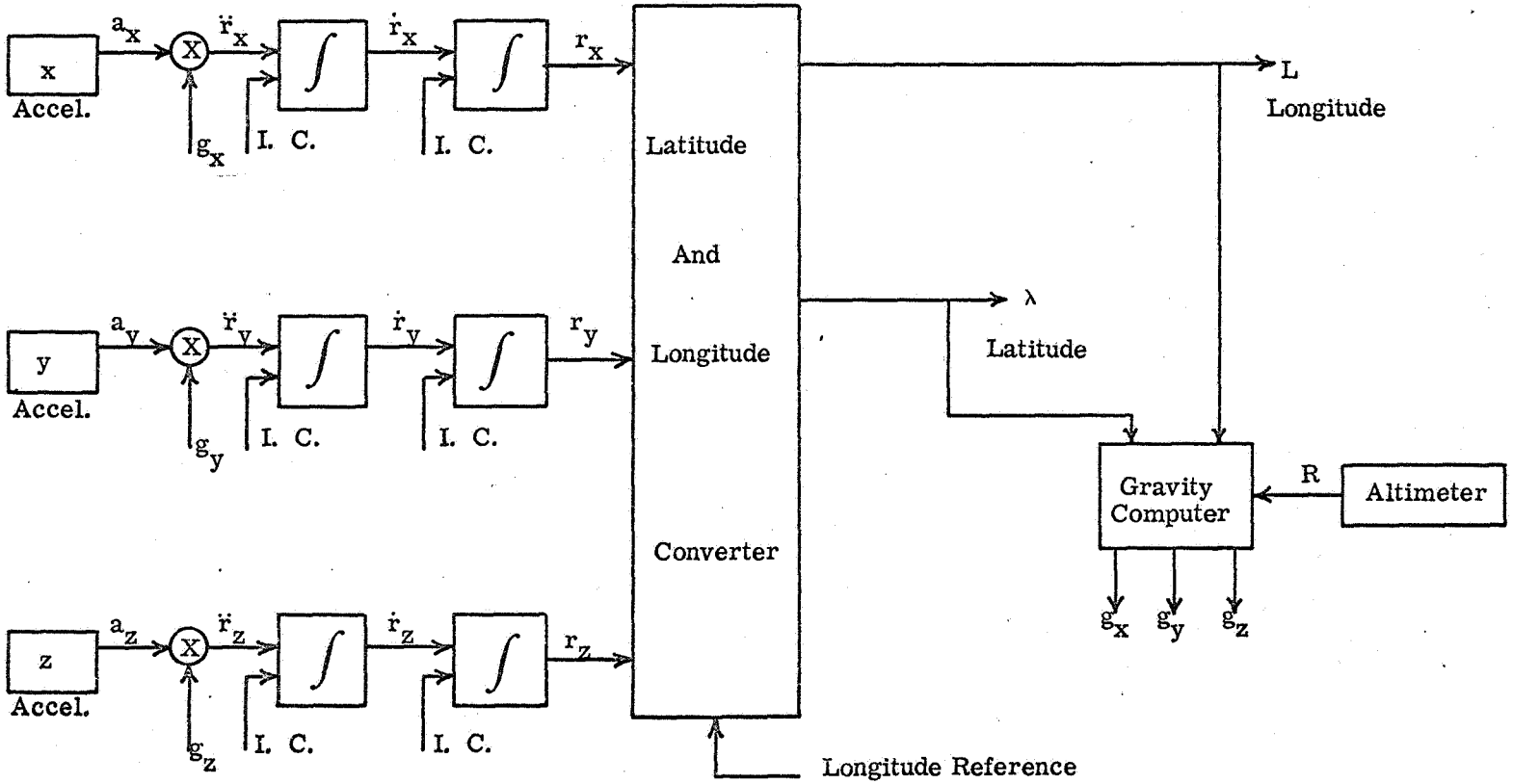

BLOCK DIAGRAM OF THE SPACE STABILIZED SYSTEM

FIG. 1-2

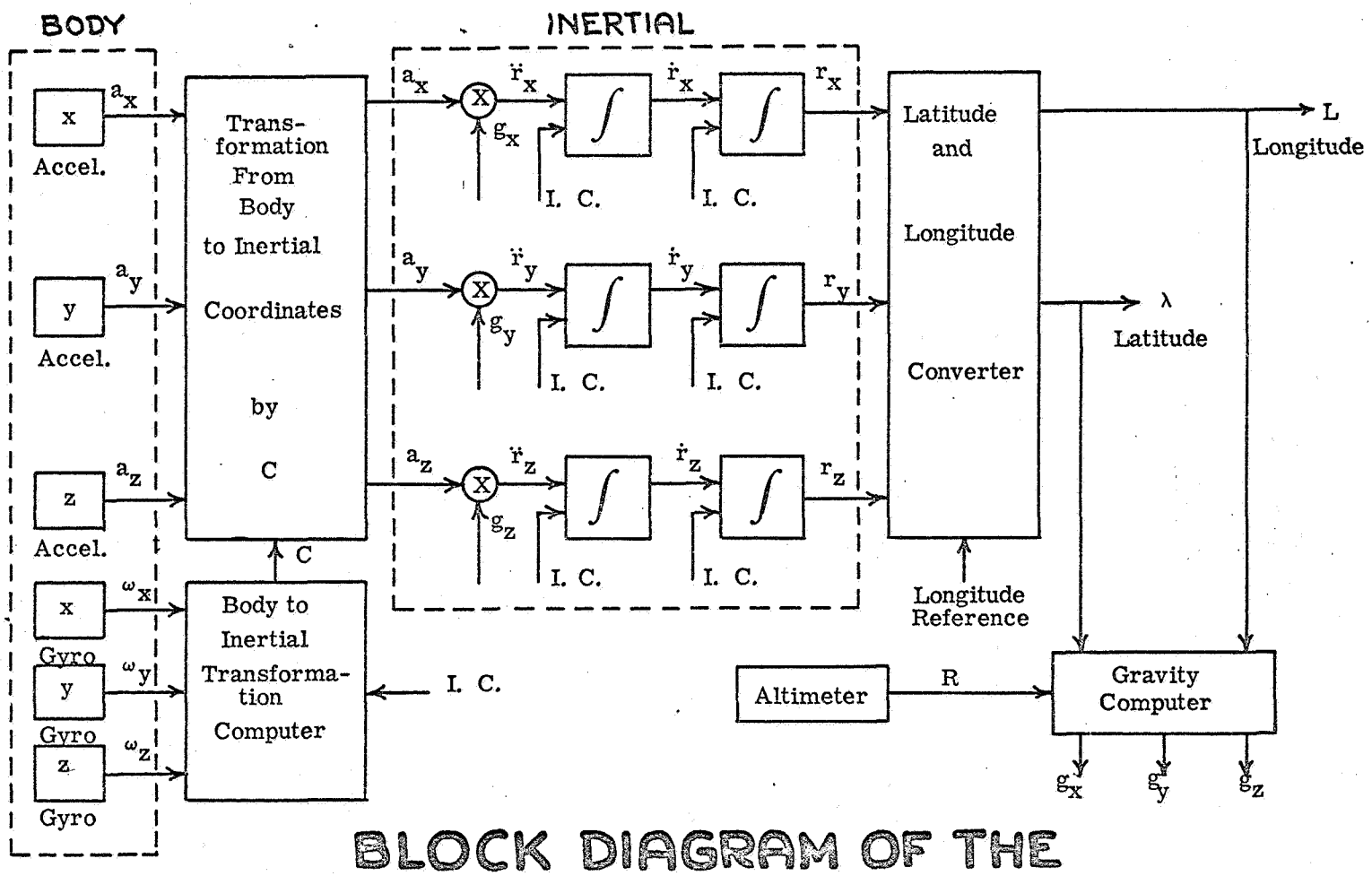

BLOCK DIAGRAM OF THE STRAPDOWN SYSTEM

FIG. 1-3

FIGURE 1-4

The space-stabilized and local-level systems' position errors for Mission #1

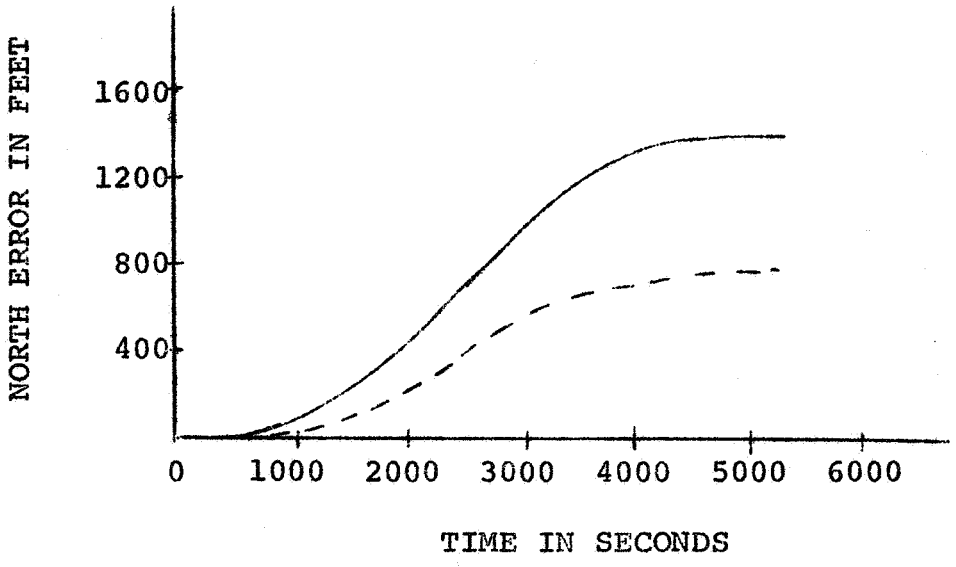

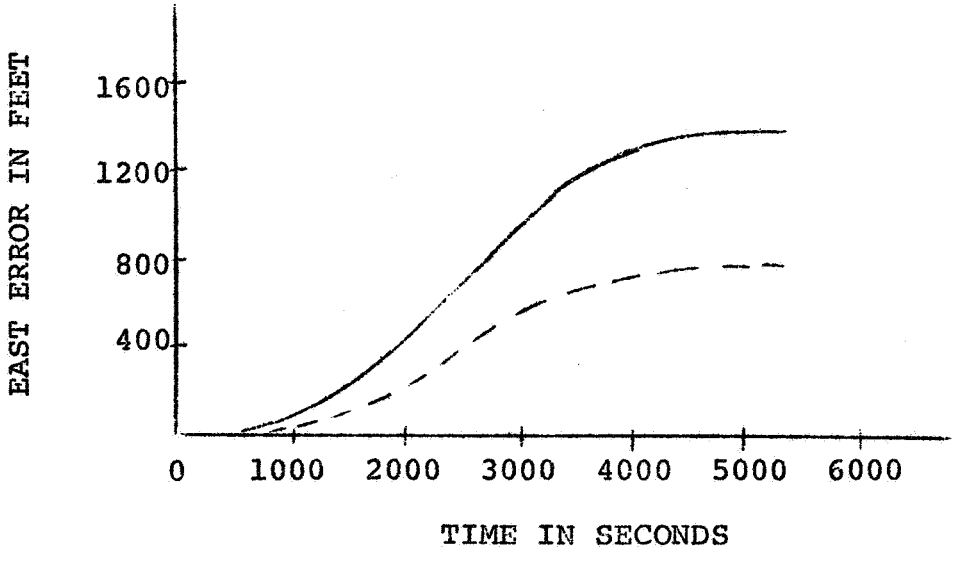

_____ represents the total RMS position error
----- represents the position error due to the bias term

FIGURE 1-5

The strap-down system's
position errors for Mission #1

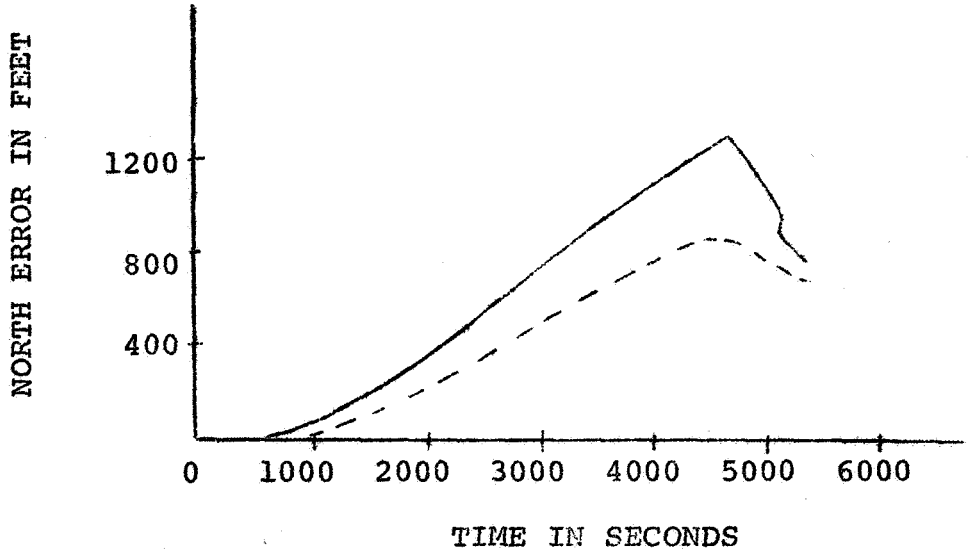

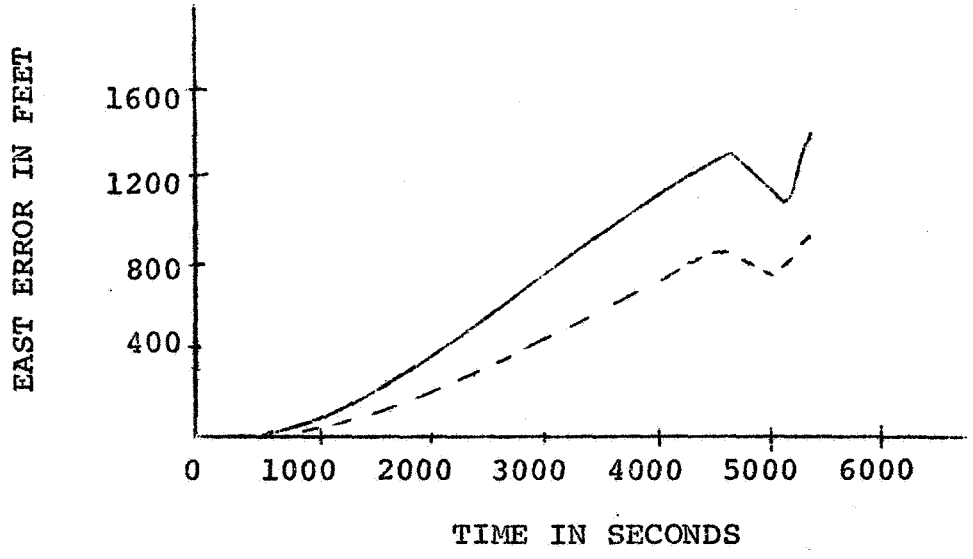

——— represents the total RMS position error
----- represents the position error due to the bias term

FIGURE 1-6

The space-stabilized and local-level systems' position errors for Mission #2

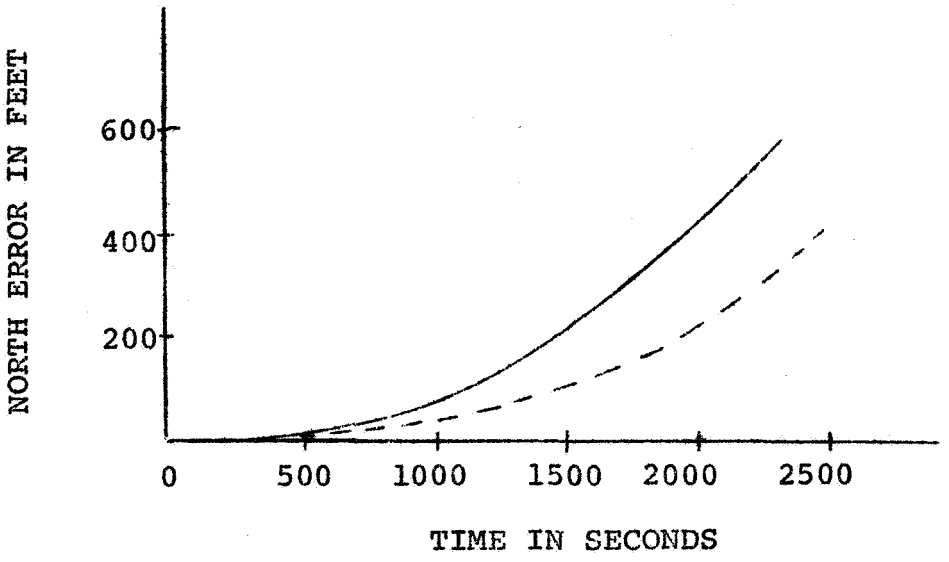

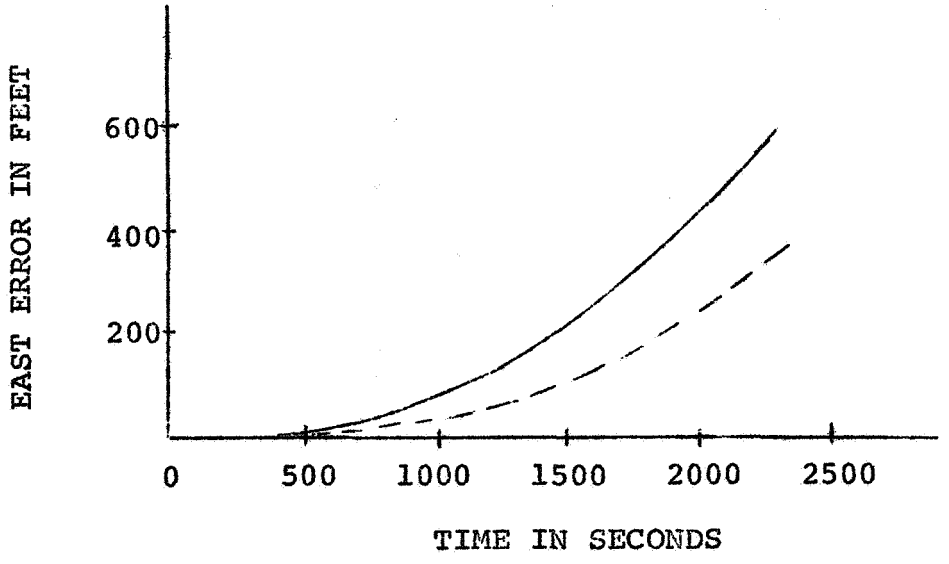

——— represents the total RMS position error
----- represents the position error due to the bias term

FIGURE 1-7

The strap-down system's
position errors for Mission #2

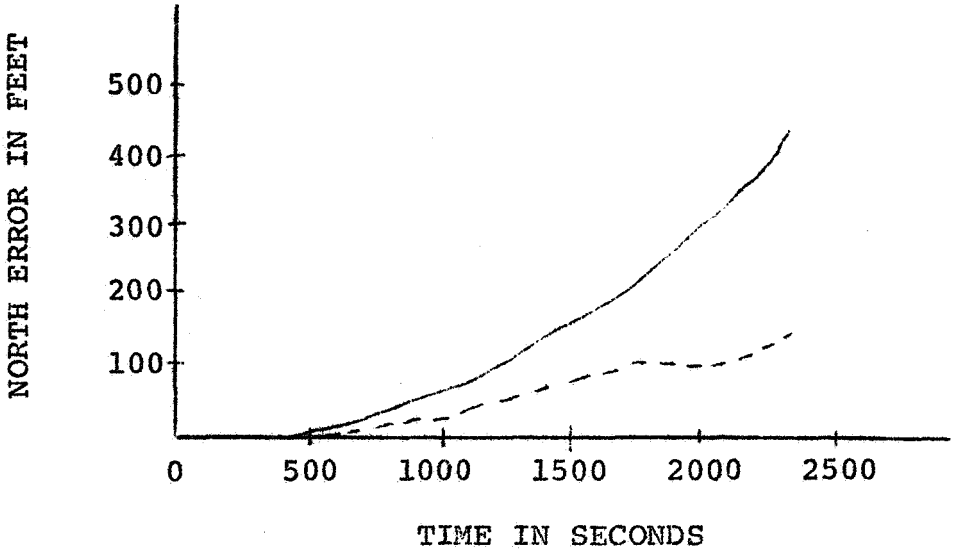

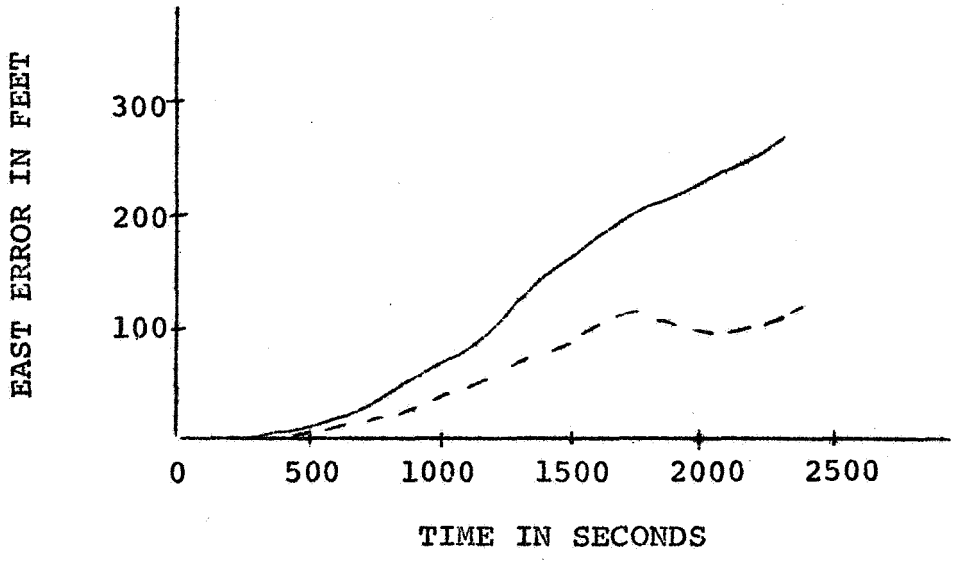

——— represents the total RMS position error
----- represents the position error due to the bias term

FIGURE 1-8

The local-level and strap-down systems' position errors for Mission #3

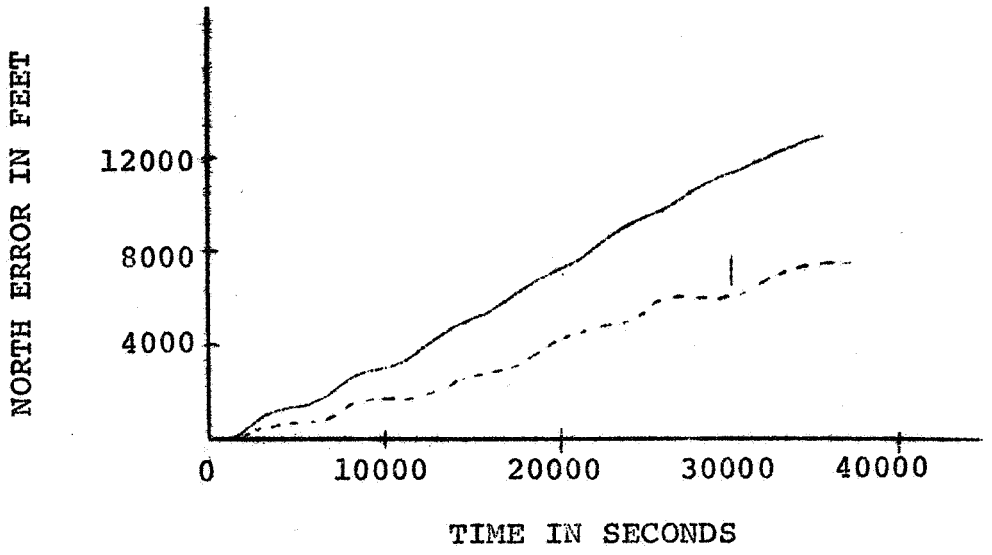

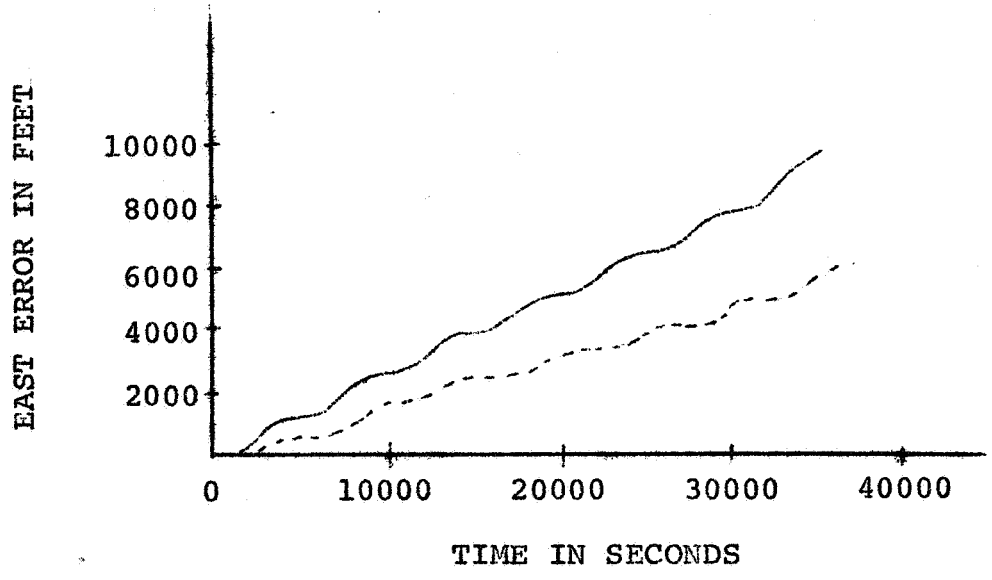

——— represents the total RMS position error
----- represents the position error due to the bias term

FIGURE 1-9

The space-stabilized system's
position errors for Mission #3

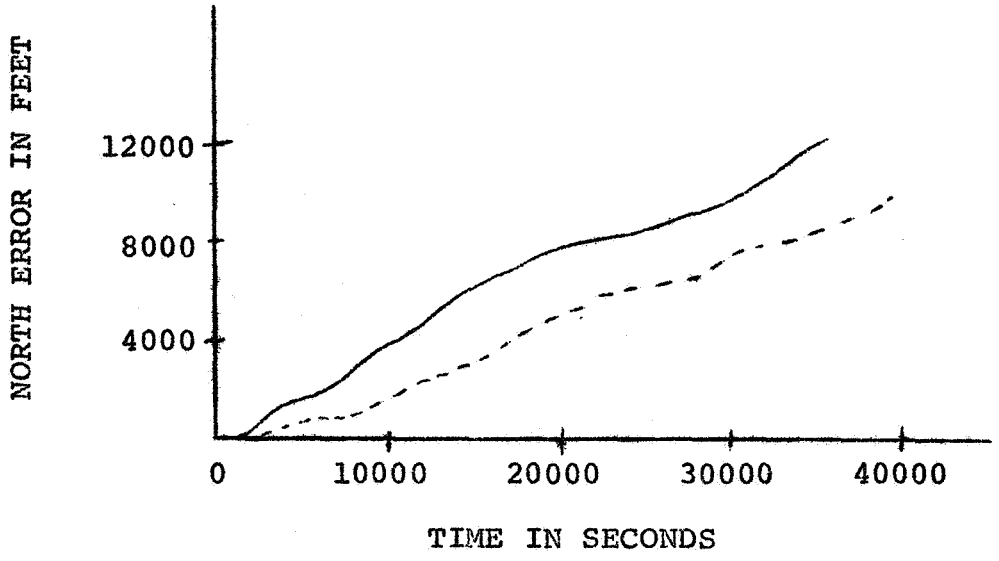

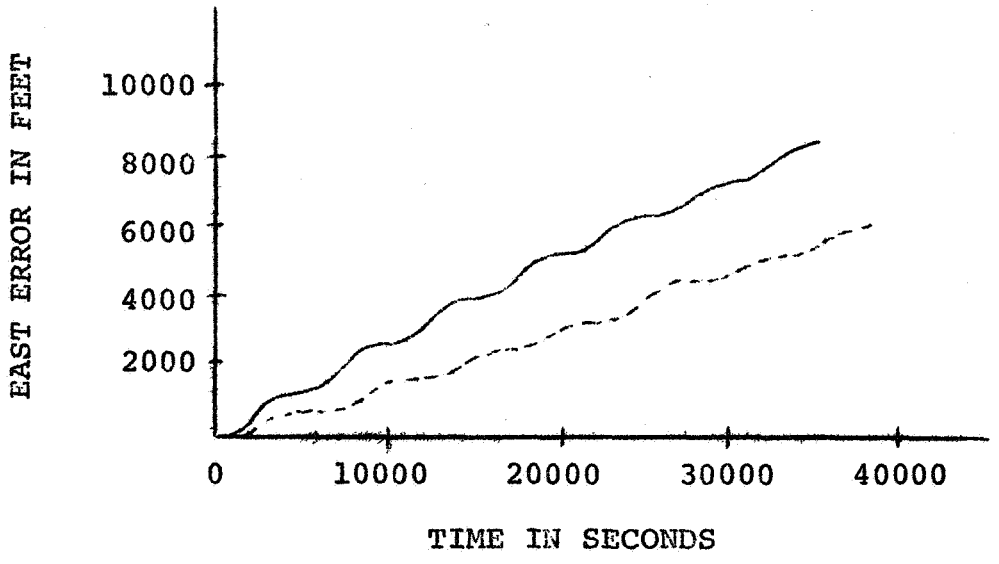

——— represents the total RMS position error
----- represents the position error due to the bias term

FIGURE 1-10

The space-stabilized and local-level systems' position errors for Mission #4

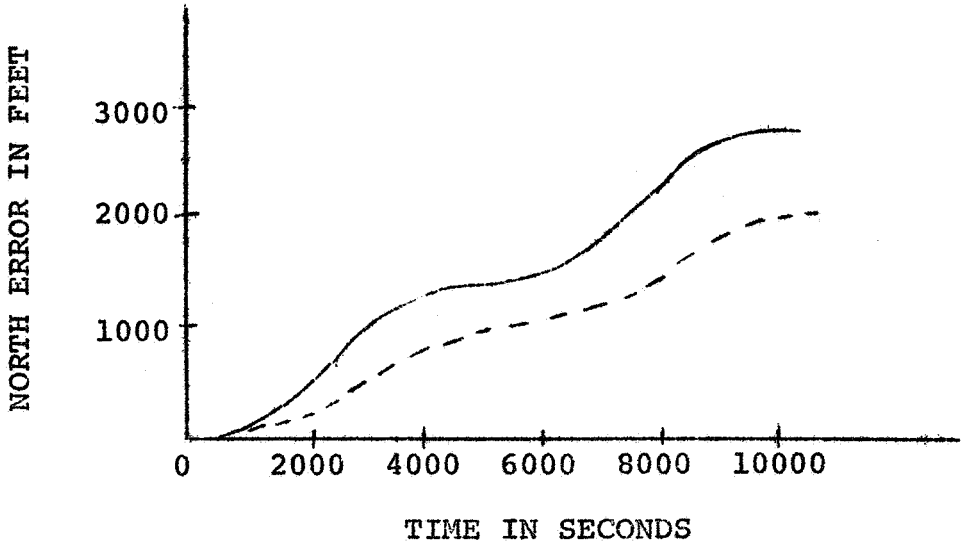

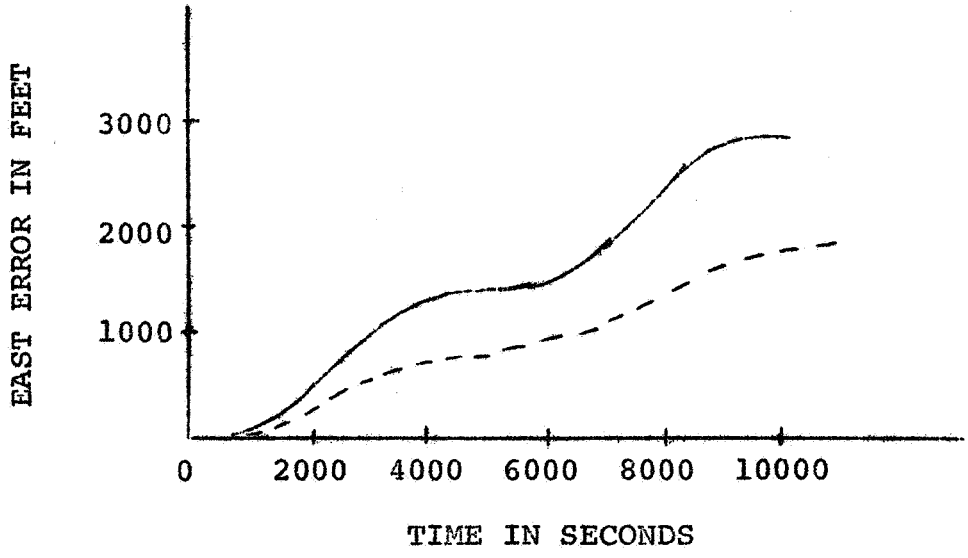

——— represents the total RMS position error
----- represents the position error due to the bias term